Determination of $LiTaO_3$ acoustic physical constants at hypersonic frequencies from bulk and surface wave velocities

2002 J. Phys.: Condens. Matter 14 545

(http://iopscience.iop.org/0953-8984/14/3/323)

INSTITUTE OF PHYSICS PUBLISHING JOURNAL OF PHYSICS: CONDENSED MATTER

J. Phys.: Condens. Matter **14** (2002) 545–553 PII: S0953-8984(02)29164-X

Determination of $LiTaO_3$ acoustic physical constants at hypersonic frequencies from bulk and surface wave velocities

V L Zhang, M H Kuok, H S Lim and S C Ng

Department of Physics, National University of Singapore, Singapore 117542, Republic of Singapore

E-mail: phykmh@nus.edu.sg

Received 26 September 2001, in final form 8 November 2001
Published 21 December 2001
Online at stacks.iop.org/JPhysCM/14/545

Abstract

Using Brillouin scattering, we have measured the velocity angular dispersion of the surface and bulk acoustic waves in X-cut and 36° Y-cut $LiTaO_3$. The complete set of twelve independent acoustic physical constants at hypersonic frequencies is evaluated using a *simultaneous* fit to only the velocity angular dispersion data on both surface Rayleigh and bulk acoustic waves. In comparison to physical constants determined in the ultrasonic frequency range, our acoustic constants yield better agreement between theory and experiment for the angular dispersion of the surface Rayleigh and second leaky wave velocities. Additionally, computation based on these acoustic constants has accurately predicted the velocity angular dispersion of the bulk waves and their scattering coefficients.

1. Introduction

$LiTaO_3$ is widely used as a substrate in surface acoustic wave (SAW) and optoelectronic devices. The design of such devices and the analysis of the propagation characteristics of acoustic waves require accurate values of the acoustic physical constants of $LiTaO_3$. However, published values of these constants [1–7] are determined mainly by ultrasonic techniques, in the MHz range instead of the desirable GHz operating range for many SAW devices. Investigations [8,9] have revealed that surface and bulk mode velocities measured by Brillouin scattering (GHz range) are systematically lower than the corresponding velocities predicted by theory, which is based on physical constants measured ultrasonically. Because of this discrepancy, and the fact that many types of SAW devices operate in the GHz range, there is a need to find a precise set of acoustic physical constants of $LiTaO_3$ using, for instance, Brillouin scattering which probes acoustic modes in this frequency region.

$LiTaO_3$ has twelve independent acoustic physical constants, namely six elastic constants at constant electric field (c_{11}^E, c_{12}^E, c_{13}^E, c_{14}^E, c_{33}^E and c_{44}^E), four piezoelectric stress constants

(e_{15}, e_{22}, e_{31} and e_{33}), and two dielectric constants at constant strain (ε_{11}^S and ε_{33}^S). There are three oft-cited sets of these constants, which are those determined by Kovacs *et al* [1], Warner *et al* [2] and Kushibiki *et al* [3] using ultrasonic techniques. Kushibiki *et al* [3] determined the latest values, with high precision, from measurements of bulk wave velocities and dielectric constants. The set obtained by Warner *et al* [2] was based on measurements of bulk wave velocities, dielectric and piezoelectric constants. Kovacs *et al* [1] obtained their values from two dielectric constants and a least-squares fit to surface wave velocities.

While numerous ultrasonic measurements of these acoustic constants have been made in the MHz range, only two Brillouin measurements, which probe waves at hypersonic frequencies, have been reported. One measurement was performed by Blachowicz and Kleszczewski [10], who determined the elastic constants from measurements of acoustic bulk mode velocities. The other, by Kuok *et al* [9], yielded a set of effective elastic constants evaluated by a fit to velocity dispersion data on bulk modes.

Previous fitting procedures [1, 4, 5, 9, 10] require, besides measured mode velocities, the measurement of dielectric and/or piezoelectric constants. In contrast, we have been able to determine the complete set of twelve independent constants from a fit to *only* mode velocities obtained by Brillouin scattering. Also, in contrast to previous fitting procedures, a *simultaneous* fit to both the surface and bulk mode velocities was performed. Additionally, no constraints were imposed on any of the values of the twelve fitting parameters—they were all allowed to vary freely. This fitting approach was found to yield good agreement between theory and experiment for both surface and bulk wave properties.

2. Experimental measurements

Optical grade $LiTaO_3$ crystals, of at least 99.99% purity, were obtained from MTI Corporation. They were in the form of polished 36° Y-cut and X-cut wafers with an orientation precision of $\pm 0.5°$. Brillouin spectra were recorded, at room temperature, using a JRS Scientific Instruments (3 + 3)-pass tandem Fabry–Pérot interferometer and the 514.5 nm line of an argon-ion laser, with a typical beam power of 120 mW incident on the sample. A stream of pure argon gas was directed at the irradiated spot on the sample to cool it and to keep air away from it. In the 180°-backscattering geometry used, the horizontal incident light wave vector $\boldsymbol{k}$ made an angle θ with the surface normal and the backscattered light was collected, using an f/2 lens, from the solid angle around $-\boldsymbol{k}$, with the sagittal plane vertical. Measurements were carried out at an incidence angle of $\theta = 70°$ over the half angular period of $0° \leqslant \phi \leqslant 90°$ on the 36° Y-cut plane, and at $\theta = 60°$ over the complete angular period of $0° \leqslant \phi \leqslant 180°$ on the X-cut plane. For surface modes, the azimuthal angle, ϕ, is the in-plane angle between the wave vector of the mode and the respective reference crystallographic axes. In the case of bulk modes, ϕ is the in-plane angle between the projection, on the X-cut plane, of the wave vector of the mode and the respective reference crystallographic axes.

The phase velocities, V, of the acoustic modes were calculated from their corresponding Brillouin frequencies, ν, using

$$V = 2\pi\nu/q \tag{1}$$

where

$$q = 4\pi \sin\theta/\lambda \qquad \text{(surface waves)} \tag{2}$$

$$q = 4\pi n/\lambda \qquad \text{(bulk waves).} \tag{3}$$

λ denotes the incident light wavelength, and n is the refractive index taken to be 2.210 [11].

In surface Brillouin scattering experiments, errors arise from geometrical aperture effects of the finite-size collection lens used, and the variation in the scattering cross section across the aperture [12, 13]. Thus a correction has to be made for these effects. In the case of our optical collection system, the measured values of surface wave velocities were raised by 1%, a correction obtained following the procedure reported by Mutti *et al* [12]. The total measurement uncertainties, arising from such error sources as determination of free-spectral-range, wave propagation direction, sample orientation, spectra fitting and heating effect, are ± 0.8, ± 2–4 and $\pm 0.4\%$ for the Rayleigh wave, the second leaky wave and the bulk modes, respectively.

We have also performed the measurement of Brillouin intensity of the bulk modes in the 90°-scattering geometry. In this geometry, the horizontal laser beam is incident at 45° on one face of a two-sided polished X-cut $LiTaO_3$ wafer and the scattered light is collected from the opposite face. The wafer was placed with either its crystallographic Z- or Y-axis vertical. Thus the light interacted with the bulk acoustic waves propagating horizontally along the respective crystallographic Y- and Z-axes. The measured intensity is taken to be the area under the Brillouin peak, after subtraction of the background intensity.

3. Results and discussion

The dependence of the respective slow transverse bulk mode (STW), fast transverse bulk mode (FTW) and the longitudinal bulk mode (LW) velocities on their propagation directions, in X-cut $LiTaO_3$, is shown in figure 1. The variations of the Rayleigh wave velocity and the second leaky wave with their propagation directions, on the X-cut plane, are presented in figures 2 and 3, respectively. The second leaky wave, which is also termed the high-frequency pseudosurface wave, leaks energy into the bulk. Because it suffers severe attenuation, it appears as a Brillouin peak with a large line width [9]. Also displayed in figures 2 and 3 are the theoretical velocities computed using the partial-wave method [14] based on the three sets of ultrasonic acoustic physical constants determined by Kovacs *et al* [1], Warner *et al* [2] and Kushibiki *et al* [3]. The experimental Rayleigh wave velocity dispersion curve parallels its theoretical curves calculated from these constants, but is systematically lower than these by 1.5%. The measured velocities of the second leaky wave are, in general, smaller than their corresponding ultrasonic ones by 2%.

The angular dispersion of the Rayleigh wave velocity on the 36° Y-cut plane is displayed in figure 4. As shown in the figure, the velocity of this wave is rather insensitive to the propagation direction on this plane. For comparison, the theoretical velocities computed using the three sets of ultrasonic constants are also presented in the figure. The measured Rayleigh wave velocity dispersion curve follows the theoretical curves well, but is also systematically lower than them, this time by about 1.5%.

Such depression of the Brillouin values (GHz range) of the SAW velocities, relative to the ultrasonic (MHz range) values, has been observed for other materials such as Ni [15], Si [16], InSb [17] and GaAs [18]. For instance, a Brillouin study by Kuok *et al* [18] of surface wave propagation on (111) GaAs has revealed that the overall discrepancies are 1.5% for the Rayleigh wave and 3% for the second leaky wave, after correcting for the systematic error introduced by the finite collection aperture. The systematic mismatch between Brillouin and ultrasonic values of the SAW velocities is a long-standing controversial issue and many reasons have been advanced to explain it. For instance, Stoddart *et al* [13] proposed that the discrepancy could be attributed to errors arising from the finite size of the collection lens used. After allowing for this correction, the discrepancies observed between the Brillouin and ultrasonic velocities of the surface modes still fall outside the experimental uncertainties and thus are believed to be real.

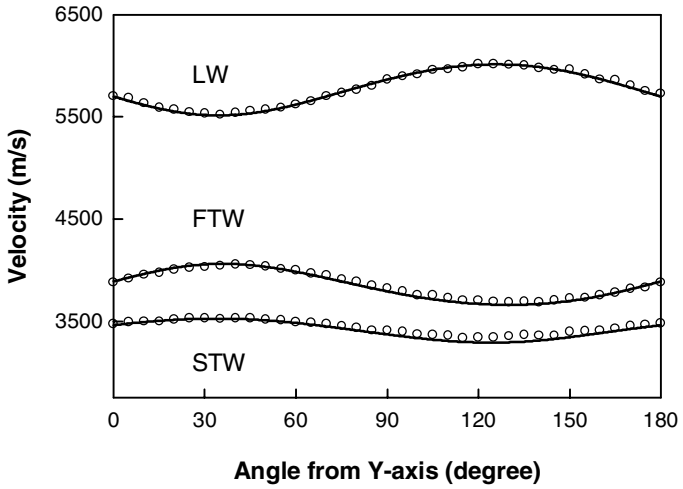

Figure 1. Angular dispersion of transverse (STW and FTW) and longitudinal (LW) bulk acoustic modes in X-cut $LiTaO_3$. The experimental data are denoted by open circles. The error bars for the measured data are smaller than the circles used to denote them. The solid curves represent the calculated velocities based on our constants.

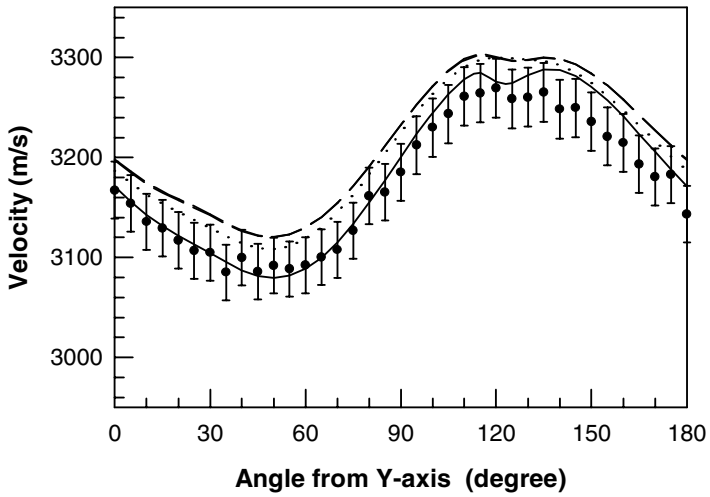

Figure 2. Angular dispersion of the Rayleigh wave on X-cut $LiTaO_3$. The experimental data are denoted by circles. Also shown are the theoretical branches based on our constants (solid curve), the constants of Warner *et al* [2] (dotted curve), and Kushibiki *et al* [3]/Kovacs *et al* [1] (dashed curve).

In this study, the density [3] of $LiTaO_3$ is taken to be 7460.4 ± 0.4 kg m^{-3}, and the twelve acoustic physical constants, namely c_{11}^E, c_{12}^E, c_{13}^E, c_{14}^E, c_{33}^E, c_{44}^E, e_{15}, e_{22}, e_{31}, e_{33}, ε_{11}^S and ε_{33}^S, were determined by a simultaneous fit to the theoretical Rayleigh, transverse and longitudinal bulk wave velocities to our experimental values. Thirty measured velocities of bulk waves as well as twelve of surface waves propagating along various directions on X-cut and 36° Y-cut $LiTaO_3$ were used for this purpose.

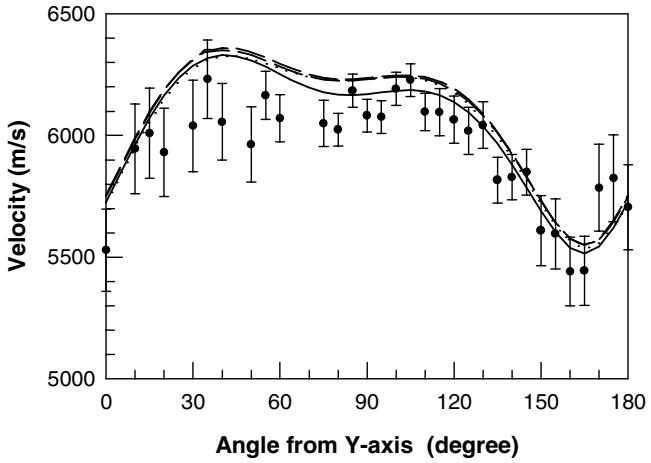

Figure 3. Angular dispersion of the second leaky wave on X-cut $LiTaO_3$. The experimental data are denoted by circles. Also shown are the theoretical branches based on our constants (solid curve), the constants of Warner *et al* [2] (dotted curve), and Kushibiki *et al* [3]/Kovacs *et al* [1] (dashed curve).

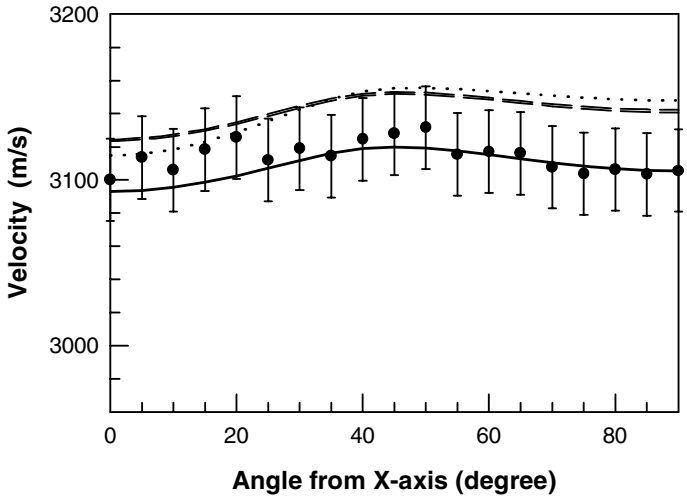

Figure 4. Angular dispersion of the Rayleigh wave on 36° Y-cut $LiTaO_3$. The experimental data are denoted by circles. Also shown are the theoretical branches based on our constants (solid curve), the constants of Warner *et al* [2] (dotted curve), and Kushibiki *et al* [3]/ Kovacs *et al* [1] (dashed curve).

We now give an outline of the fitting procedure used. We consider a set of N measurements of acoustic wave velocities $V_i^{\exp}(i = 1, 2, \ldots, N)$ with corresponding propagating directions described by x_i, each subject to some random error due to the finite precision of the measurement process. Given the standard deviation, σ_i, of each data point, then the best-fit parameters, $\boldsymbol{a} \equiv \{a_1, a_2, \ldots, a_m\}$, can be determined by minimizing the quantity

$$\chi^2(\boldsymbol{a}) = \sum_{i=1}^{N} \left(\frac{V_i^{\exp} - V_i^{\mathrm{th}}(x_i; \boldsymbol{a})}{\sigma_i} \right)^2 . \tag{4}$$

Table 1. Brillouin and ultrasonic values of acoustic physical constants for $LiTaO_3$.

		Present study	Ref. [2]	Ref. [3]	Ref. [1]
Elastic	c_{11}^E	23.24 ± 0.24	23.3	23.305 ± 0.004	23.28 ± 0.36
constant	c_{12}^E	4.67 ± 0.29	4.7	4.644 ± 0.006	4.65 ± 0.46
(10^{10} Pa)	c_{13}^E	8.41 ± 0.85	8.0	8.346 ± 0.067	8.36 ± 0.43
	c_{14}^E	-1.27 ± 0.15	-1.1	-1.075 ± 0.004	-1.05 ± 0.02
	c_{33}^E	26.82 ± 1.56	27.5	27.522 ± 0.114	27.59 ± 0.50
	c_{44}^E	9.39 ± 0.63	9.4	9.526 ± 0.002	9.49 ± 0.04
Piezoelectric	e_{15}	2.69 ± 0.22	2.6	2.628 ± 0.022	2.64 ± 0.27
	e_{22}	1.62 ± 0.30	1.6	1.831 ± 0.015	1.86 ± 0.10
stress constant	e_{31}	-0.55 ± 1.08	0.0	-0.145 ± 0.067	-0.22 ± 0.28
(C m^{-2})	e_{33}	1.99 ± 0.81	1.9	1.849 ± 0.118	1.70 ± 0.55
Dielectric	ε_{11}^S	40.67 ± 6.22	41	41.9 ± 0.4	40.9 ± 3.9
constant (ε_0)	ε_{33}^S	42.29 ± 6.25	43	41.8 ± 0.4	42.5 ± 2.6

In our case, the number of parameters, m, equals twelve, while the total number, N, of experimental data used in the fit is 42. These 42 experimental velocities were chosen so that they are evenly spread over a wide range of propagation directions. It was found that a larger fitting database resulted in only a marginal decrease in χ^2, with parameters that are essentially the same as those obtained using the 42 data points. V_i^{th} are the theoretical wave velocities, which are functions of the twelve parameters, computed using the partial-wave method described by Farnell [14]. The nonlinear least-squares Levenberg–Marquardt method [19] was employed for the curve fitting. This approach allows for a smooth variation between two extreme procedures: the steepest descent and the Hessian method. The Hessian is a matrix of second derivatives of χ^2 with respect to the fitting parameters $(\partial^2\chi^2/\partial a_i \partial a_j)$. When χ^2 is far from the minimum, the method of steepest descent is employed. As χ^2 approaches the minimum, the algorithm switches to the Hessian method to compute the best fit. Given trial values for the parameters, the Levenberg–Marquardt procedure was applied iteratively to improve the trial solution until the difference between two consecutive χ^2 is less than a specified convergence tolerance. We used the set of acoustical constants from Warner *et al* [2] as our initial trial values. Subsequent trial values were then generated by adding a random number, which varies from -5 to 5, to each of the constants.

The values of the twelve acoustic physical constants that yield the best fit are listed in table 1. For comparison, the constants reported by Kovacs *et al* [1], Warner *et al* [2] and Kushibiki *et al* [3] are also included in the table. Our fitted elastic constants are generally smaller than these. This is not unexpected as wave velocities measured by Brillouin scattering are generally lower than those determined by ultrasonic means. Relative to the elastic constants of Kovacs *et al* [1], this discrepancy varies from 0.2%, for c_{11}^E, to as large as 21% for c_{14}^E. In contrast, our piezoelectric stress constant, e_{31}, is significantly larger than the corresponding values evaluated by Kovacs *et al* [1] and Kushibiki *et al* [3]. Interestingly, Kovacs *et al* [1] had to rely on measured values of the dielectric constants, as they thought that it was not possible to obtain all twelve physical constants from a fit to surface wave velocities alone. In our fitting approach, the only measured quantity required is the acoustic mode velocity. Also, no constraint was imposed on any of the twelve parameters. Despite this, our fitted values of the dielectric constants, ε_{11}^S and ε_{33}^S, are in good agreement with experiment.

In their Brillouin investigation, Kuok *et al* [9] used only effective elastic constants as fitting parameters where, unlike in the present study, the piezoelectric and dielectric constants were not considered as separate fitting parameters and their fitting routine was confined to bulk modes. By measuring the bulk mode velocities in three crystallographic directions, Blachowicz and Kleszczewski [10], determined the elastic constants c_{11}, c_{33} and c_{44} directly and the other elastic constants indirectly. They took piezoelectricity into account. Their elastic constants are generally lower than ours and, in particular, their c_{13} value is 39% smaller.

The angular dispersion of the Rayleigh, transverse and longitudinal bulk acoustic mode velocities, based on this set of acoustic physical constants, was computed using the partial-wave method [14]. These results, together with the corresponding experimental velocities, are displayed in figure 4 for the Rayleigh wave on the 36° Y-cut surface, figure 2 for the Rayleigh wave on the X-cut surface as well as figure 1 for the transverse and longitudinal bulk modes in X-cut $LiTaO_3$. It is clear from these figures that our set of constants, when compared to the other ultrasonic constants, produces the best fit to the experimental data determined at hypersonic frequencies. In particular, figure 2 shows that our theoretical dispersion curve can accurately reproduce the fine double-hump feature, in the $110^\circ \leqslant \phi \leqslant 140^\circ$ region, of the experimental curve for the Rayleigh mode on the X-cut surface. However, while these results are reassuring, they are to be expected, as the new constants were extracted from these Brillouin data.

To ascertain whether the new set of constants is indeed a better one for hypersonic-frequency data, we use it in the computation of the second leaky wave velocities on the X-cut surface as they were not used in the determination of these constants. The calculated velocity of this wave is plotted as a function of its propagation direction in figure 3. Although the figure reveals that all four theoretical curves are parallel the experimental curve, it is the theoretical curve, computed using our set of physical constants, that is closest to the experimental curve, especially in the $80^\circ \leqslant \phi \leqslant 130^\circ$ region where the measurement precision is highest. The curves, based on the three sets of ultrasonic constants, lie further above the experimental curve. Once again the Brillouin velocity, in this case for the second leaky wave, is depressed relative to the ultrasonic value.

In particular, we consider the second leaky wave travelling in the 112° direction, relative to the crystallographic Y-axis. This direction chosen as the X-112°Y cut of $LiTaO_3$ is commonly used in the fabrication of SAW devices of GHz frequency. Our Brillouin measurement has recorded a velocity of 6096 ± 80 m s^{-1}. The corresponding values derived from constants determined by Kovacs *et al* [1], Warner *et al* [2] and Kushibiki *et al* [3] are 6226, 6220 and 6235 m s^{-1}, respectively. In comparison, calculations using our hypersonic-frequency physical constants yield a velocity of 6176 m s^{-1}, which agrees best with the experimental value.

As a further test of the accuracy of the hypersonic constants, we have considered the measured intensity of light scattered from bulk acoustic waves by computing the scattering coefficient [20] which can be expressed as

$$R = \frac{\pi^2 k_B T}{\lambda^4 \rho V^2} \frac{n_i}{n_s} \frac{1}{\cos^2\theta_i \cos^2\theta_s} \sum_{j,l=1}^{3} (\Phi_{jl}\alpha_j\beta_l)^2 \tag{5}$$

where V is the velocity of the acoustic wave of given polarization, k_B is the Boltzmann constant, T is the temperature of the crystal, n_i and n_s are the refractive indices in the directions of the incident and scattered light, θ_i and θ_s are the angles between the electric field vector and the dielectric displacement vector of the respective incident and scattered light of given polarization, and α_j and β_l define the polarization states of the scattered and incident light. The tensor $\Phi_{jl} = \sum_{m,n=1}^{3} n_j^2 n_l^2 p_{jlmn} q_m \gamma_n$, where p_{jlmn} is the Pockels photoelastic tensor, and q_m and γ_n are the components of the respective propagation vector and polarization vector of

Table 2. Calculated wave velocities, ratios of scattering coefficients and measured Brillouin intensities for p–p polarized scattering from bulk modes in X-cut $LiTaO_3$ along the Y-axis and Z-axis.

	Wave velocity ($m\ s^{-1}$)		Scattering coefficient (in units of R_L)	Brillouin intensity (in units of I_L)[c]
	Theory	Experiment	Theory	Experiment
Y-axis				
Pure transverse	3527	3528[d]	0[a]	0.0
Quasi transverse	3827	3820	0.66[a]	0.7
Quasi longitudinal	5723	5759	1[a]	1
Z-axis				
Pure transverse	3548	3547[d]	0[b]	0.0
Pure transverse	3548	3547[d]	0.01[b]	0.0
Pure longitudinal	6113	6130	1[b]	1

[a] $R_L = 22.8\pi^2 k_B n^8 T\lambda^{-4} 10^{-15}\ m^{-1}$.
[b] $R_L = 8.6\pi^2 k_B n^8 T\lambda^{-4} 10^{-15}\ m^{-1}$.
[c] I_L = Brillouin intensity of the longitudinal mode.
[d] Data from p–s polarized spectrum.

the acoustic wave. The rotational contributions to the scattering coefficients have been taken into account following the theoretical procedure of Nelson and Lax [21]. The photoelastic constant data used in our calculation were obtained from [22].

The measured bulk mode intensities, in p–p polarization, are listed in table 2, where they are presented as intensity ratios relative to the intensity of the longitudinal bulk mode. For comparison, the theoretical scattering coefficients, in the p–p polarization, as well as the calculated and measured bulk mode velocities along the respective Y- and Z-axes in X-cut $LiTaO_3$ are listed in table 2. It can be seen that agreement between theory and experiment is excellent, again confirming the accuracy of our acoustic constants.

4. Conclusion

The velocity angular dispersion of the Rayleigh, second leaky and bulk waves in $LiTaO_3$ has been measured by Brillouin scattering. A set of twelve acoustic physical constants for $LiTaO_3$ was determined from a simultaneous fit to the velocity angular dispersion data of the Rayleigh and bulk acoustic waves. This consistent set of constants is able to reproduce accurately the velocity dispersion curves of the Rayleigh, second leaky and bulk acoustic modes as well as the scattering coefficients of the bulk modes. As the frequency of each of the surface and bulk modes involves a different combination of the acoustic constants, the inclusion of both modes in the fit can provide corroborative information on the constants. The results discussed in this paper clearly exemplify such a situation. Since a discrepancy between Brillouin and ultrasonic velocities was found for surface waves, our set of constants could be more appropriate than the ultrasonic constants, for the design and the analysis of propagation characteristics of acoustic waves on $LiTaO_3$-substrate SAW devices operating in the GHz range.

Acknowledgments

This research was supported by the National University of Singapore under project No R-144-000-018-112 and through the award of a research scholarship to V L Zhang.

References

[1] Kovacs G, Anhorn M, Engan H E, Visintini G and Ruppel C C W 1990 *Proc. IEEE Ultrason. Symp.* **1** 435
[2] Warner A W, Onoe M and Coquin G A 1967 *J. Acoust. Soc. Am.* **42** 1223
[3] Kushibiki J, Takanaga I, Arakawa M and Sannomiya T 1999 *IEEE Trans. Ultrason. Ferroelectr. Freq. Control* **46** 1315
[4] Taki K and Shimizu Y 1994 *Japan. J. Appl. Phys.* **33** 2976
[5] Murota M and Shimizu Y 1991 *Japan. J. Appl. Phys.* (Suppl 30-1) **30** 156
[6] Takanaga I and Kushibiki J 1999 *J. Appl. Phys.* **86** 3342
[7] Smith R T 1967 *Appl. Phys. Lett.* **11** 146
[8] Blachowicz T and Kleszczewski Z 1997 *Arch. Acoust.* **22** 351
[9] Kuok M H, Ng S C, Zhang V L and Fan H J 2001 *Appl. Phys. Lett.***78** 607
[10] Blachowicz T and Kleszczewski Z 1998 *J. Acoust. Soc. Am.* **104** 3356
[11] Gervais F and Fonseca V 1998 *Handbook of Optical Constants of Solids* vol 3, ed E D Palik (Orlando, FL: Academic) p 777
[12] Mutti P, Bottani C E, Ghislotti G, Beghi M, Briggs G A D and Sandercock J R 1994 *Advances in Acoustic Microscopy* vol 1, ed A Briggs (New York: Plenum) ch 7
[13] Stoddart P R, Crowhurst J C, Every A G and Comins J D 1998 *J. Opt. Soc. Am.* **15** 2481
[14] Farnell G W 1970 *Physical Acoustics* vol 6, ed W P Mason and R N Thurston (New York: Academic) p 109
[15] Mendik M, Sathish S, Kulik A, Gremaud G and Wachter P 1992 *J. Appl. Phys.* **71** 2830
[16] Kuok M H, Ng S C, Rang Z L and Liu T 1999 *Solid State Commun.* **110** 185
[17] Kuok M H, Ng S C and Zhang V L 2000 *Appl. Phys. Lett.* **77** 1298
[18] Kuok M H, Ng S C and Zhang V L 2001 *J. Appl. Phys.* **89** 7899
[19] Wong S S M 1992 *Computational Methods in Physics and Engineering* (Englewood Cliffs, NJ: Prentice-Hall) p 373
[20] Fabelinskii L 1968 *Molecular Scattering of Light* ed R T Beyer (New York: Plenum) p 143
[21] Nelson D F and Lax M 1970 *Phys. Rev. Lett.* **24** 379
[22] Dixon R W 2000 *CRC Handbook of Chemistry and Physics: a Ready-reference Book of Chemical and Physical Data* vol 12, ed D R Lide, 81st edn (Boca Raton, FL: CRC Press) p 159